Sol-gel prepared nanoscopic metal fluorides – a new class of tunable acid-base catalysts

S. Wuttke[a], S. M. Coman[a, b], J. Kröhnert[c], F.C. Jentoft[c, d] and E. Kemnitz[a]*

[a] Humboldt-Universität zu Berlin, Institut für Chemie, Brook-Taylor-Str. 2, 12489 Berlin, Germany.
[b] University of Bucharest, Faculty of Chemistry, Department of Chemical Technology and Catalysis, Bdul Regina Elisabeta 4-12, 030016 Bucharest, Romania.
[c] Fritz-Haber-Institut der Max-Planck-Gesellschaft, Abteilung Anorganische Chemie, Faradayweg 4-6, 14195 Berlin, Germany.
[d] University of Oklahoma, Chemical, Biological and Materials Engineering, 100 East Boyd St., Norman, OK 73019, USA.

* Corresponding author: e-mail erhard.kemnitz@chemie.hu-berlin.de,
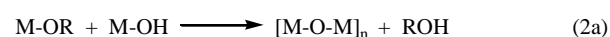
Abstract

In this article, the high potential of the fluorolytic sol-gel process to synthesise nanoscopic metal fluorides with different acid-base properties is shown. These nanoscopic materials exhibit high potential to be used as heterogeneous catalysts due to their high surface areas and their tunable surface properties. Thus, for each specific reaction the required surface properties of the catalysts can be "adjusted" to achieve a high yield and selectivity of the desired product. As a consequence, a greener method of chemical production can be accomplished. Moreover the cheap and easy synthesis of the catalysts using basic chemicals makes them not only interesting for fundamental research but provides an easy transformation to industrial applications.

Keywords: sol–gel, heterogeneous catalysis, metal fluorides, acidity and basicity

1. Introduction

The sol-gel (solution-gelation) process has become one of the most important routes for preparing porous materials. In general, it is a versatile solution-based process that starts from a molecular precursor and is characterized by the formation of a clear sol (colloidal suspension of solid particles with particle diameters < 200 nm) which then may be converted into a viscous gel. This might be an aerogel or xerogel depending on the method of the solvent removal used. Supercritical drying allows removing the solvent without significantly changing the gel network structure and this results in an aerogel. On the other hand, a xerogel will be obtained when removing the solvent by common evaporation, which is typically accompanied by a significant rate of shrinkage and densification.

Sol-gel synthesis usually results in the formation of metal oxides [1-2]. This route is based on the reaction of a metal alkoxide dissolved in alcoholic solution and water. The reaction is considered to proceed in two different steps: hydrolysis (eqn. 1) and condensation (eqn. 2a and b).

$$\text{M-OR} + \text{H}_2\text{O} \longrightarrow \text{M-OH} + \text{ROH} \qquad (1)$$

$$\text{M-OR} + \text{M-OH} \longrightarrow [\text{M-O-M}]_n + \text{ROH} \qquad (2a)$$

$$\text{M-OH} + \text{M-OH} \longrightarrow [\text{M-O-M}]_n + \text{H}_2\text{O} \qquad (2b)$$

In most cases, the condensation reactions are incomplete, and hence, result in materials with a significant amount of alcoholate groups. Therefore, a post-calcination step up to 450°C is required in order to obtain metal oxide phases that are free of organic contaminations. Materials

Sol-gel prepared nanoscopic metal fluorides – a new class of tunable acid-base catalysts, S. Wuttke et al..,
Catalysis Today 152 (2010), 2-10

2

prepared in this way have been successfully applied as heterogonous catalysts in numerous basic reactions.

In 2003, an analogue sol-gel synthesis, denoted as "fluorolytic" sol-gel synthesis, was developed for metal fluorides [3]. Here, the metal alkoxide dissolved in an appropriate organic solvent, reacts with anhydrous HF instead of water and therefore undergoes a fluorolysis as described by eqn 3:

$$M\text{-}OR + HF \longrightarrow M\text{-}F + ROH \qquad (3)$$

The limited fluorolysis reaction rate in combination with the donating organic solvent molecules prevents the formation of ordered solids. In contrast to the oxide synthesis the formation of metal-fluorine-metal bridges resulting in nanoscopic metal fluoride particles occurs without condensation [4].

As in the case of metal oxides the reaction usually remains incomplete, the extent being dependent on the metal used, and consequently, a post-fluorination is necessary. However, this can be done by a post fluorination under gentle conditions (100 to 250°C). By this method, highly disordered metal fluorides with very high surface areas can be synthesised. Particular properties of these materials are the significantly increased Lewis acidity in comparison to conventionally prepared metal fluorides. For example, high surface area (HS-) AlF_3 is one of the strongest known solid Lewis acids [5-6]. Another interesting example is MgF_2 which usually is a neutral solid. However, the nanoscopic HS-MgF_2 exhibits medium strong Lewis acidity due to undercoordinated Mg^{2+} on the surface [7-8]. It has been shown that the Lewis acidity of HS-AlF_3 is too strong for several organic reactions resulting in the formation of by-products [9]. On the other hand, the Lewis acidity of HS-MgF_2 is too weak to provide sufficient activity [10]. To overcome this problem, ternary fluorides were synthesised. These systems consist of a minor component (5-20 mol%), the guest, and a major component, the host. Applying the Tanabe model [11] to binary metal fluoride systems, suggests the generation of Lewis acidity for CrF_3/MgF_2 or FeF_3/MgF_2, whereby in both cases MgF_2 acts as the host [12]. Therefore, the possibility of tuning pure Lewis acidic metal fluoride systems and applying them as heterogeneous catalysts has been successfully proven [13-14]. Hence, with pure sol-gel prepared nanoscopic metal fluorides and binary metal fluoride systems pure Lewis acidic metal fluorides of different strengths are accessible which can be applied in heterogeneous catalysis.

We also need to consider reactions that require catalysts with Brønsted acid surface sites or basic sites. For those reactions we have further developed the application of the fluorolytic sol-gel-synthesis route in order to access a new class of bi-functional heterogeneous catalysts. Two different approaches will be presented that on one hand result in different Lewis acid/Brønsted-base materials and on the other hand in different Lewis/Brønsted acidic materials. Moreover, we will show that these acid-base sites can be tuned over a range and can therefore be "adjusted" for a specific reaction, which will be demonstrated in the synthesis of (all-*rac*)-α-tocopherol (Vitamin E).

2. Experimental

2.1. Sample preparation

2.1.1. Synthesis of magnesium oxide fluorides.

50 ml dry methanol was added to 1.56 g magnesium metal (Aldrich, 99.98%) in a round-bottom flask with a reflux condenser for 3 h. An understoichiometric amount of HF (n_1 = 102 mmol for $MgF_{1.6}O_{0.2}$ as soon as n_2 = 26 mmol for $MgF_{0.4}O_{0.8}$) dissolved in MeOH was added to the obtained $Mg(OCH_3)_2$ solution. After adding to this solution the necessary amount of distilled water (V_1 = 1ml; n = 52 mmol and V_2 = 3.7 ml; n = 207 mmol respectively) and aging for 12 h, the final gels were dried under vacuum at T = 70 °C for 5 h. The dry powder obtained in this way was treated in argon for 3 h at 350 °C.

2.1.2.Synthesis of hydroxylated magnesium fluorides.

A range of five magnesium fluoride catalysts were prepared from metallic Mg, using a sol-gel method, as follows: 1.56 g (64 mmol) metallic Mg (Aldrich, 99.98%) was reacted with 50 ml dry methanol at room temperature overnight. After heating under reflux conditions for 3 h a stoichiometric amount of 130 mmol HF dissolved in various amounts of water (HF solution concentrations: 20wt% HF, 40wt% HF, 57wt% HF, 71wt% HF and 87wt% HF) was added to the formed $Mg(OCH_3)_2$ solution. The mixture reacted to a highly viscous transparent gel. After aging for 12 h, the gel was dried under vacuum at room temperature. The formed solid product was then dried further under vacuum at 70 °C, for 5 h. Prepared catalysts were named: MgF_2-20, MgF_2-40, MgF_2-57, MgF_2-71 and MgF_2-87.

2.1.3. Synthesis of (all-*rac*)-α-tocopherol.

Catalytic tests were carried out in glass vials with a standard capacity of 8 ml, at 100 °C, under vigorous stirring (1500 rpm), using 6 ml of heptane /propylene carbonate (50/50 (v/v)) mixture. The amount of used catalyst was 50 or 200 mg and the amount of reactants 152 or 304 mg TMHQ and 0.4 ml IP (corresponding to TMHQ/IP molar ratio of 1/1 and 2/1). After the catalyst separation from the two-phase solvent mixture, the heptane phase containing the tocopherol was separated and the solvent removed under vacuum to give a crude product. Analyses of crude product were performed with HPLC (column – EC 125/4.6 NUCLEOSIL 120-5 C18; eluent: acetonitrile; flow rate: 0.8 ml / min; wavelength: 280 nm; volume sample: 15 μl), and 1H-, 13C-NMR (*Bruker AV 400*) spectrometer, in $CDCl_3$

Sol-gel prepared nanoscopic metal fluorides – a new class of tunable acid-base catalysts, S. Wuttke et al..,
Catalysis Today 152 (2010), 2-10

3

solvent and Me$_4$Si as internal standard). Trimethylhydroquinone (97 wt.%) and isophytol (95 wt.%) were purchased from Acros Organics. The other reagents (analytical grade) were obtained from Merck.

2.2. Characterisation

2.2.1. FTIR-measurements

The IR spectra shown in Figs. 2, 4 and 5 were recorded with the apparatus and following the procedures described in [23]. After the CO adsorption experiment, the magnesium oxide fluorides were again treated under vacuum at 573 K for 2 h. After this reactivation the sample was treated with stepwise increasing pressure of CO$_2$.

The IR spectra shown in Figs. 9 and 10 were acquired using a Perkin Elmer S 2000 with a spectral resolution of 4 cm^{-1}. The sample was pressed into a self-supporting wafer with an area weight of 15 mg/cm^2. The wafer was placed in a stainless steel, low temperature infrared cell with CaF$_2$ windows. The sample was activated in the IR cell under vacuum at different temperature for 24 h. After activation the sample was cooled using liquid N$_2$ in the presence of an inert gas (He, 2 hPa) to 77 K. The CO pressure was increased stepwise. The spectra are shown as difference of the spectrum of the sample in presence of CO minus the spectrum of the sample before CO dosage.

2.2.2. ^{1}H MAS NMR.

Solid state MAS NMR experiments were done on a Bruker AVANCE 400 spectrometer using a 4 mm rotor for ^{1}H ($v_{Larmor}(^1H)$ = 400.1 MHz) with the appropriate Bruker MAS probe heads and applying different spinning frequencies. The spectrometer was calibrated with standard reference substances (^{1}H: adamantane as secondary standard δ_{iso}(CH2) = 29.5 ppm and δ_{iso}(H) = 1.79 ppm against TMS).

3. Results and discussion

3.1. Metal (hydr)oxide fluorides

The different sol-gel synthesis approaches as described above result either in the formation of pure metal oxides or pure metal fluorides. Both synthesis routes have in common to start from a suitable metal alkoxide that undergoes a reaction either with water (hydrolysis) in the case of metal oxides, or a reaction with anhydrous hydrogen fluoride (fluorolysis) in the case of metal fluorides. Thus, we explored the possibility to combine both reaction routes to synthesise metal oxide fluorides by employing in a first reaction step understoichiometric amounts of anhydrous HF in order to perform selectively the fluorolysis followed by
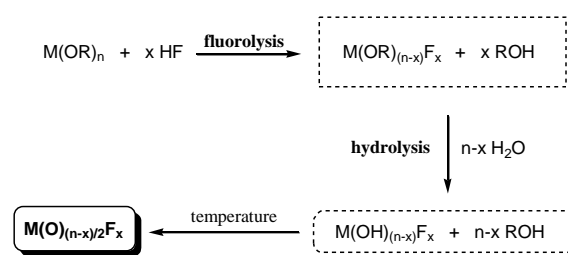

Fig. 1: Diagram of the synthesis of metal oxide fluorides.

the addition of the stoichiometrically required amount of water to finish the conversion of the remaining M-OR-groups. The obtained solid, after calcination at a certain temperature, should be a metal oxide fluoride. This process is schematically illustrated in Fig. 1. Moreover depending on the amount of anhydrous HF used (x in Fig. 1 is variable), metal oxide fluorides of different fluorine to oxygen ratios should be obtained.

This general process has been already successfully applied for the synthesis of magnesium oxide fluoride catalysts for Michael addition reactions [15]. Starting from magnesium methoxide and varying the x in Fig. 1, metal oxide fluorides with different oxygen to fluorine ratios were prepared. The bulk structure and the catalytic data for their application as heterogeneous catalysts in the Michael additions were also reported in the before mentioned article. It turned out that pure magnesium oxide and magnesium oxide fluorides with high oxygen contents are very active catalysts in Michael additions but exhibit low selectivity towards the desired addition product. By decreasing the oxygen content and consequently increasing fluorine content in the magnesium oxide fluorides the activity decreases but the selectivity increases significantly. An optimum was found for the catalyst with an F to Mg molar ratio of 1.6 [15].

Little has been reported about the acid-base properties of these magnesium oxide fluorides. Hence, the surface acidity and basicity of these materials were investigated in more detail in order to better understand their exciting catalytic properties. Consequently, FTIR spectroscopic studies using different probe molecules have been performed. From the various compositions, two representative different magnesium oxide fluorides were used to exemplify their characteristics. The one sample with a high fluorine content, F : Mg molar ratio of 1.6, is designated as to MgF$_{1.6}$O$_{0.2}$. The other sample with a low fluorine content, F : Mg molar ratio of 0.4, is designated as to MgF$_{0.4}$O$_{0.8}$. That means, there is a magnesium oxide fluoride with a stoichiometry close to that of magnesium fluoride (MgF$_{1.6}$O$_{0.2}$) whereas the other one is close to magnesium oxide (MgF$_{0.4}$O$_{0.8}$).

Carbon monoxide, CO, is a very suitable probe molecule for the characterisation of acid surface sites. By interaction of CO with a surface acid site, the linear (CO) stretching vibration is shifted towards higher wave numbers
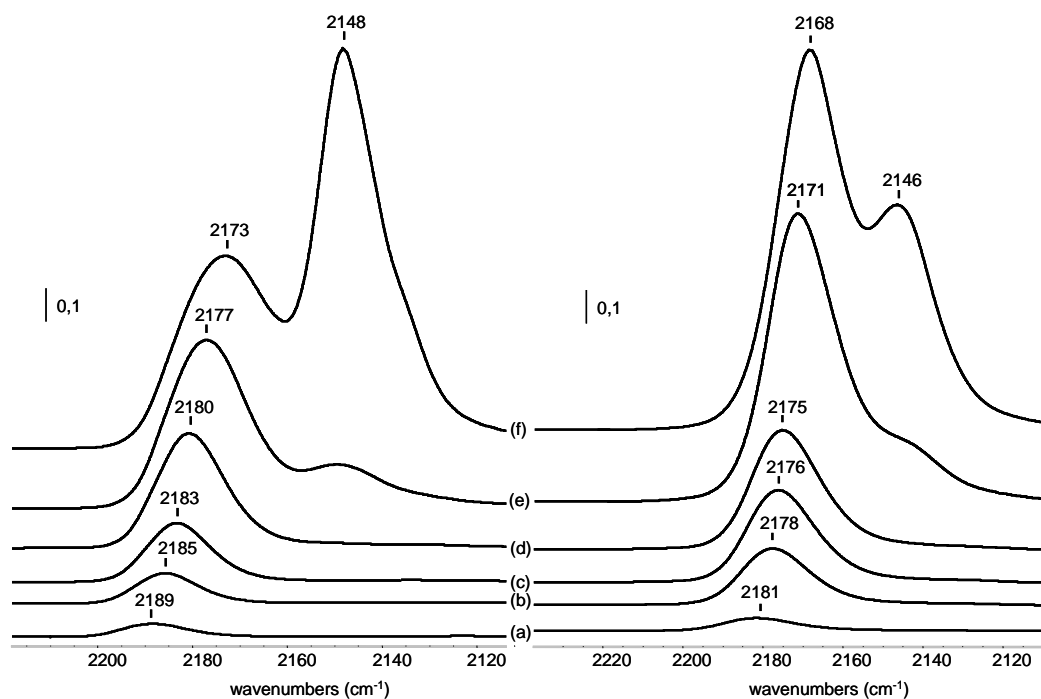
Sol-gel prepared nanoscopic metal fluorides – a new class of tunable acid-base catalysts, S. Wuttke et al..,
Catalysis Today 152 (2010), 2-10

4

Fig. 2: IR difference spectra recorded at 100 K of $MgF_{1.6}O_{0.2}$ (left) and $MgF_{0.4}O_{0.8}$ (right) outgassed at 573 K followed by increasing doses of CO (spectra a to e) until finally an equilibrium pressure of CO was established (1 torr, spectra f). Spectra are normalized to the same sample mass.

as compared to gaseous CO [5]. The higher this shift, the higher is the acidity of the specific surface site.

The difference IR spectra of the CO stretching region of CO adsorbed on $MgF_{1.6}O_{0.2}$ and $MgF_{0.4}O_{0.8}$ are given in Figure 2. Both samples show very similar characteristics. For $MgF_{1.6}O_{0.2}$, the maximum of the CO band at low coverage is found at 2189 cm^{-1}, whereas for $MgF_{0.4}O_{0.8}$, the maximum of the CO band is found at 2181 cm^{-1} at the same coverage. Providing higher amounts of CO increases the intensity of these bands, whereas the maximum shifts downwards to 2173 cm^{-1} for $MgF_{1.6}O_{0.2}$ and 2168 cm^{-1} for $MgF_{0.4}O_{0.8}$, respectively. Simultaneously, at high coverage of CO a second band appears in both cases in the range of about 2148-2146 cm^{-1} (spectra Fig. 2e and f). This band region which appears at high coverage of CO can be clearly assigned to physisorbed CO on the surface. The bands in the range of 2170-2190 cm^{-1} can be assigned to medium Lewis acid sites on the surface. The very important fact in this regard is that at the same coverage of CO different shifts are observed for the samples. Spectra of CO adsorbed on the sample $MgF_{1.6}O_{0.2}$ show a slightly higher blue shift than the sample $MgF_{0.4}O_{0.8}$. This result can be rationalized in two ways.

The first explanation is that the materials may exhibit different undercoordinated Mg-sites at the surface, or alternatively, that both have the same undercoordinated Mg-sites but linked to different ligands. Spoto et al. reported [16] about the interaction of adsorbed CO on MgO. Three different undercoordinated sites were assigned to three different CO frequencies.

A band centred at 2200 cm^{-1} was assigned to three-fold coordinated magnesium (Mg_{3c}^{2+}), the band centred at 2159 cm^{-1} was assigned to four-fold coordinated magnesium (Mg_{4c}^{2+}) and the band centred at 2152 cm^{-1} was assigned to five-fold coordinated magnesium (Mg_{5c}^{2+}). It must be pointed out that the detection of Mg_{5c}^{2+} is only possible at very low temperatures (T ~ 60 K) [16]. In the present work, the higher temperature (T ~ 100 K) that was used during the CO experiment makes the detection of this site impossible. Therefore, the main band of both samples is assigned to CO adsorbed on Mg_{4c}^{2+} . The blue shift of four-fold coordinated magnesium on the magnesium oxide fluorides is stronger than it is in the case of magnesium oxide. This is obviously due to the stronger inductive effect of fluorine atoms in comparison to oxygen atoms. In Fig. 3 a five-fold coordinated surface magnesium site with an accessible Lewis acid site on MgO (Fig. 3a) and MgF$_2$ (Fig. 3b) schematically is shown.

Due to the stronger electronegative fluorine atoms at MgF$_2$ in comparison to oxygen at MgO, the Lewis acid site in MgF$_2$ is stronger than that in MgO. This explains why Mg_{4c}^{2+} at the magnesium oxide fluorides are stronger than at magnesium oxide, but also why Mg_{4c}^{2+} at $MgF_{1.6}O_{0.2}$ is stronger than at $MgF_{0.4}O_{0.8}$. It was already shown [15] that the composition of the MgX$_6$ octahedral units is changing with the fluorine to oxygen ratio. Hence, magnesium oxide fluorides with high fluorine content like $MgF_{1.6}O_{0.2}$ are built up by fluorine-rich and oxygen-poor MgX$_6$ octahedral

Sol-gel prepared nanoscopic metal fluorides – a new class of tunable acid-base catalysts, S. Wuttke et al..,
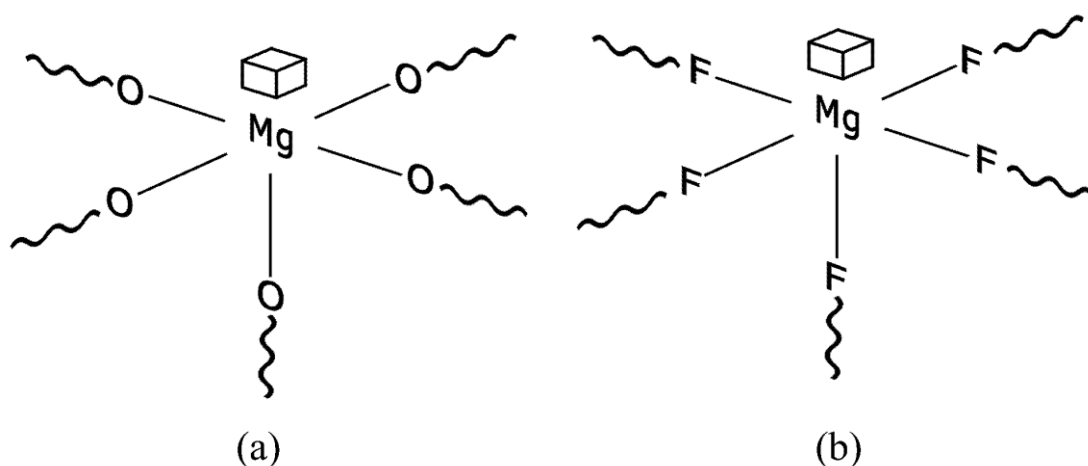Catalysis Today 152 (2010), 2-10

5

Fig.3: Accessible Lewis acid site on (a) MgO and (b) MgF_2.

units (X=F/O). Conversely, magnesium oxide fluorides with low fluorine content like $MgF_{0.4}O_{0.8}$ are built up by fluorine-poor and oxygen-rich MgX_6 octahedral units. In spite of this functionality it is understandable that the Lewis acid sites of $MgF_{1.6}O_{0.2}$ are slightly stronger than of $MgF_{0.4}O_{0.8}$.

CO_2 is a weak acidic molecule and it is used to characterise specifically basic sites of metal oxides. With basic oxygen ions, CO_2 can form different kinds of carbonate species, whereas with basic hydroxyl groups different hydrogen carbonate species will be formed [REF???].

Evacuation of the investigated sample at increasing temperatures and subsequent recording of IR spectra gives an insight into the stability of the different species which is related to the base strength of the samples [18]. Consequently, CO_2 was used as a probe molecule for the characterisation of the basic sites at the surface of the magnesium oxide fluorides.

FTIR spectra of adsorbed CO_2 show one sharp band in the range of 2355-2365 cm^{-1} (Fig. 4a) that can be ascribed to the interaction of linearly adsorbed CO_2 molecules on Lewis acid sites (undercoordinated Mg^{2+}) [19].
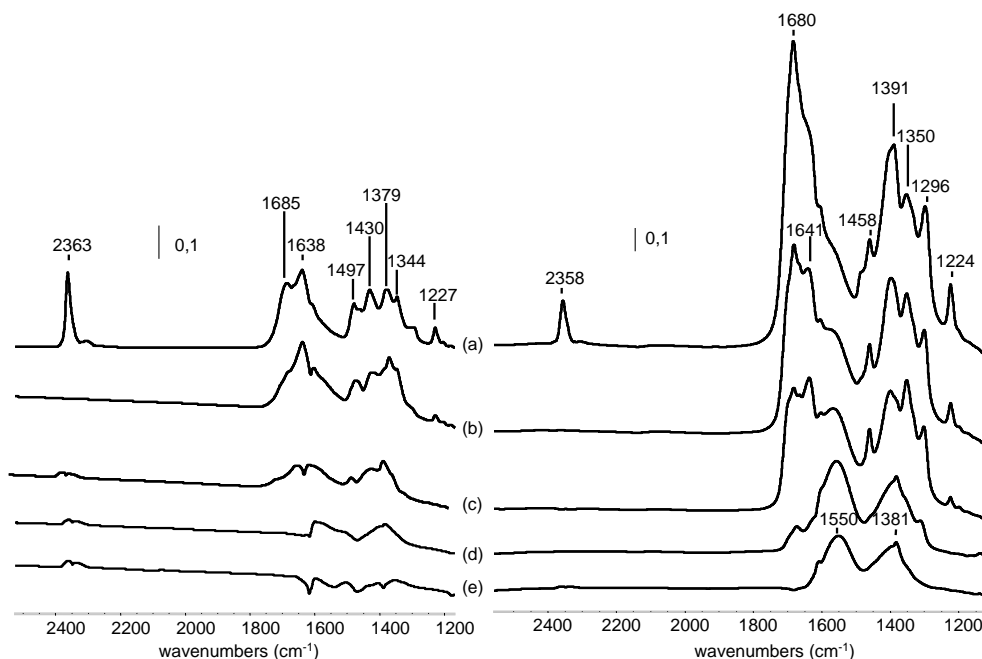

Fig. 4: IR difference spectra recorded at 298 K of $MgF_{1.6}O_{0.2}$ (left) and $MgF_{0.4}O_{0.8}$ (right) outgassed at 573 K and then after introduction of an equilibrium pressure of CO_2 (1 torr, spectra a) and consecutive desorption under vacuum at (b) T_1 = 298 K, (c) T_2 = 373 K, (d) T_3 = 473 K and (e) T_4 = 573 K for each case with 15 min. Spectra are normalized to the same sample mass.
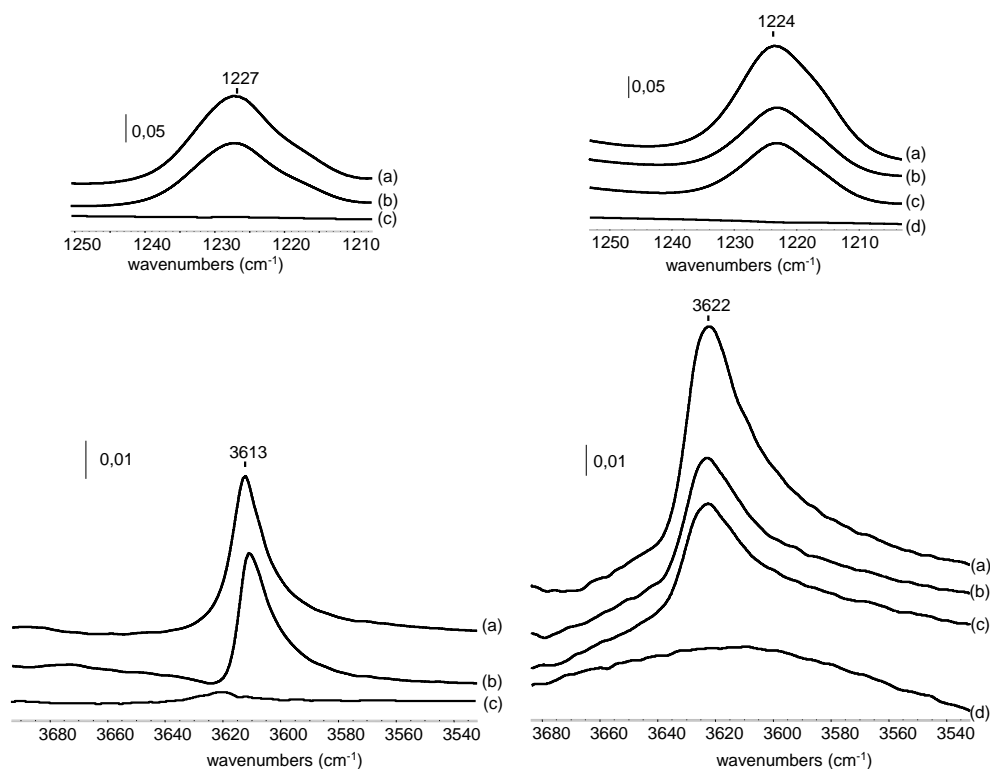
Sol-gel prepared nanoscopic metal fluorides – a new class of tunable acid-base catalysts, S. Wuttke et al..,
Catalysis Today 152 (2010), 2-10

6

Fig. 5: IR difference spectra of the $\nu(OH)$ und $\delta(OH)$ stretching region of $MgF_{1.6}O_{0.2}$ (left) and $MgF_{0.4}O_{0.8}$ (right) recorded at 298 K, outgassed at 573 K followed by addition of CO_2 until establishing an equilibrium pressure of CO_2 (1 torr, spectra a) and consecutive desorption under vacuum at (b) $T_1 = 298$ K, (c) $T_2 = 373$ K and (d) $T_3 = 473$ K for each case with 15 min. Spectra are normalized to the same sample mass.

After evacuation at ambient temperatures (Fig. 4b) this band completely disappears indicating a weak interaction. On the other hand, the range of 1700-1200 cm^{-1} is quite complex with numerous bands. In Fig. 5a both samples show two sharp and intense bands at 3613 and 1227 cm^{-1} for $MgF_{1.6}O_{0.2}$ and 3622 and 1224 cm^{-1} for $MgF_{0.4}O_{0.8}$, assigned to the $\nu(OH)$ and $\delta(OH)$ modes. Hence both samples form one hydrogen carbonate species, which comes from the presence of an OH-group on the surface. After the samples are degassed at 573 K both spectra show one sharp and intensive band at 3725 cm^{-1} (not shown), which can clearly be assigned to a terminal OH-group [20-21].

The stability of the formed hydrogen carbonate species varies. On $MgF_{1.6}O_{0.2}$ the $\nu(OH)$ and $\delta(OH)$ type are observed up to 298 K (Fig. 5b), whereas on $MgF_{0.4}O_{0.8}$ these bands are observed up to 373 K (Fig. 5c). This indicates that the OH-group on $MgF_{0.4}O_{0.8}$ is stronger basic than that on the other sample. Consequently the other bands in the range of 1700-1300 cm^{-1} are due to various, not so easily assignable bicarbonate species (Fig. 4). More importantly, from Fig. 4 it can clearly be seen that the bicarbonate species on $MgF_{0.4}O_{0.8}$ are more stable against temperature than those on $MgF_{1.6}O_{0.2}$. This means, the basic oxygen centres in $MgF_{0.4}O_{0.8}$ are stronger than in $MgF_{1.6}O_{0.2}$. The stronger basicity of $MgF_{0.4}O_{0.8}$ is evidently a result of the reduced electron withdrawing effect by the minor fluorine population in comparison to $MgF_{1.6}O_{0.2}$ thus

enabling an easier proton attraction by the more negatively charged oxygen atoms in the former compound. As already mentioned above, the MgX_6 octahedral units (X=F,O) in $MgF_{1.6}O_{0.2}$ are fluorine-rich and oxygen-poor as opposed to $MgF_{0.4}O_{0.8}$. Due to the stronger inductive effect of fluorine atoms in comparison to oxygen atoms the basic sites on $MgF_{1.6}O_{0.2}$ are weaker than on $MgF_{0.4}O_{0.8}$.

In summary it can be stated that by increasing the fluorine content of the magnesium oxide fluoride, the Lewis acidity increases whereas the basicity decreases. Therefore these sites can be tuned over a wide range thus giving access to optimised catalytic activity and selectivity of these phases as was already proven for Michael additions [15].

3.2. Hydroxylated Metal fluorides

When a metal alkoxide is reacted with stoichiometric amounts of aqueous HF a competition between fluorolysis and hydrolysis has to be expected, resulting consequently in the formation of hydroxofluorides. The F to OH ratio in the products formed this way should depend on the free Gibbs enthalpy of each reaction and on the reaction rate. In fact both, the thermodynamic data as well as the reaction rate (the fluorolysis rate for the Mg-system is about 10 times higher than the hydrolysis rate) let expect the domi

Sol-gel prepared nanoscopic metal fluorides – a new class of tunable acid-base catalysts, S. Wuttke et al..,
Catalysis Today 152 (2010), 2-10

7

nant formation of the metal fluoride [22]. However, by varying the H_2O to HF-ratio in the hydrofluoric acid differently hydroxylated metal fluoride phases should be obtained. This competitive reaction system is schematically illustrated in Fig. 6. Thus, the simultaneous fluorolysis and hydrolysis reaction leads to partly hydroxylated aluminium or magnesium fluorides, respectively, as has been already demonstrated [9, 23]. The amount of the hydroxyl groups can be adjusted to very small numbers (x < 0.1) confirming that the fluorolysis is the dominant reaction. However, as a big surprise these hydroxyl groups are Brønsted acidic in nature [9, 23].
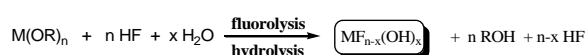
$$M(OR)_n \ + \ n\,HF \ + \ x\,H_2O \ \xrightarrow[\textbf{hydrolysis}]{\textbf{fluorolysis}} \ \boxed{MF_{n-x}(OH)_x} \ + \ n\,ROH \ + \ n\text{-}x\,HF$$

Fig. 6: Reaction path of the synthesis of hydroxylated metal fluorides.

That is astonishing because we would normally expect the hydrolysis of an $Mg\text{-}OCH_3$ bond to result in a Brønsted basic Mg-OH group as is commonly known for magnesium hydroxide [20, 21, 24].

How can the Brønsted acidic character of hydroxyl groups in magnesium fluoride prepared via the fluorolytic sol-gel-approach be rationalized?

First of all, ^{19}F-MAS-NMR spectra clearly indicate the presence of $Mg(F_{6-x}O_x)$ octahedra in these phases. When x is very small (x<0.1) the OH-groups are connected to Mg-atoms with a significantly reduced electron density due to the strong electron withdrawing power of the strongly electronegative F atoms. This obviously causes a shift of the electron density of the O-H-bond into the Mg-O-bond thus weakening the former one (Fig. 7a). As a result, the proton donor ability becomes drastically increased resulting in Brønsted acidic character of this Mg-OH-group. Secondly, as shown already above, the fluorolytic sol-gel route results in strongly distorted hydroxofluoride phases carrying a remarkable share of undercoordinated magnesium (Lewis acidic) sites. In addition, an OH-group may interact with a neighboured Lewis acid site at the surface (Fig. 7b), which also may further weaken the O-H-bond. The possibility of a "dangling" OH-group on a metal fluorine surface has already been shown based on DFT calculations [25].

On the other hand, since fluorolysis and hydrolysis reactions are proceeding simultaneously bridging OH-groups (Fig. 7c) may be formed too. It is well documented that bridging OH-groups are stronger Brønsted acid sites than non-bridging ones [26-27]. Even a contribution from the possible formation of hydrogen bonds between the H of an OH-group and a neighbouring F atom (Fig. 7d) can not be ruled out.

To confirm the result of Brønsted acidic OH-groups on a MgF_2 surface high-resolution magic angle spinning (MAS) ^{1}H NMR spectroscopy was performed on hydroxylated MgF_2. Fig. 8 shows a representative ^{1}H MAS NMR spectrum of MgF_2-71 (the number 71 indicates the percentage of the aqueous HF used). The isotropic chemical shift of $\delta = 4.8$ ppm can be assigned to remaining water on the surface and/or bulk [28].
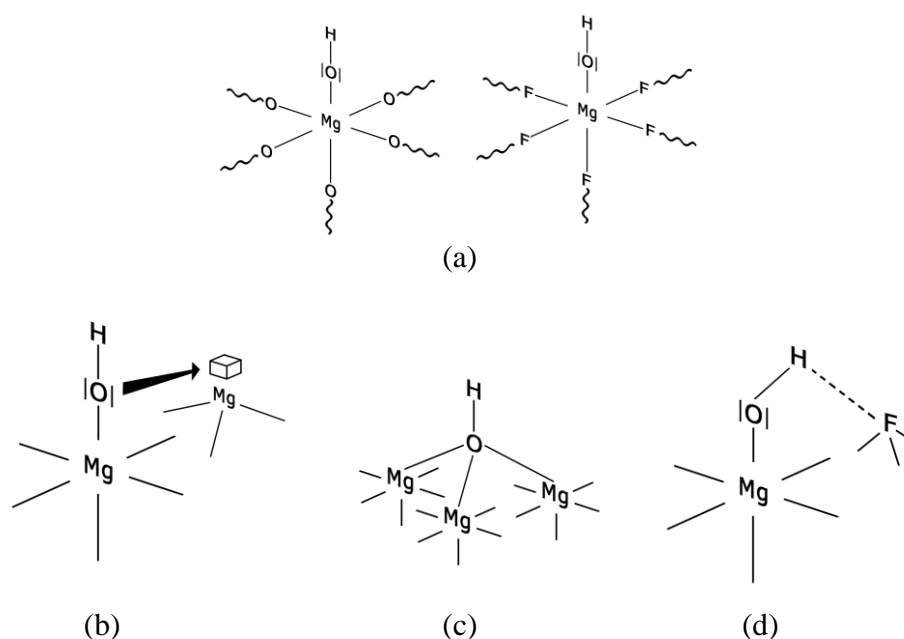

(a)

(b)   (c)   (d)

Fig. 7: Schematic representations of OH-groups in different topological situations, (a) OH-group at a MgO and MgF_2 surface, (b) interaction of a Mg-OH-group with a Lewis acid site, (c) a branched Mg-OH-group and (d) hydrogen bonding between the H of an OH-group and a neighbouring F atom.
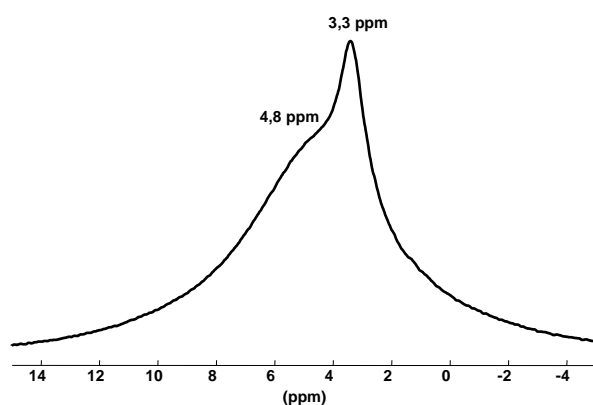
Sol-gel prepared nanoscopic metal fluorides – a new class of tunable acid-base catalysts, S. Wuttke et al..,
Catalysis Today 152 (2010), 2-10

8

Fig. 8: ^{1}H MAS NMR spectrum of MgF$_2$-71

Interestingly enough, the central signal at $\delta = 3.3$ ppm has never been observed for MgO [29] or magnesium oxofluoride before [30]. DFT calculations of ^{1}H MAS NMR chemical shifts were performed for OH-groups on MgO surfaces [29]. According to these DFT-calculations, a ^{1}H MAS NMR isotropic chemical shift of $\delta = 3.3$ ppm in the MgO sample would represent an acidic OH-group. Basic OH-groups were calculated and experimentally determined to be in the range of $\delta = 0$ to -2 ppm. Therefore, our ^{1}H MAS NMR results indicate the presence of Brønsted acidic OH-group in the sample MgF$_2$-71.

The probe molecule CO does not only interact with Lewis but also with Brønsted acid sites. When CO is interacting with OH groups, the position of the linear ν(CO) stretching vibration is blue-shifted to the range 2150-2170 cm^{-1} [5], and simultaneously the ν(OH) vibration is red-shifted due to the perturbation by CO [31].

A problem with CO adsorption measurements on hydroxylated magnesium fluoride arises from remaining water on the surface. The thermal lability of the samples does not allow for activation at elevated temperatures [23]. The MgF2-71 sample was treated in vacuum for about 24 h at 25°C or for 1–2.5 h at 70–100°C. An intense absorption feature between 3700 and 2900 cm^{-1} in the IR spectra indicated that the samples were still highly hydrated after these treatments.

Series of spectra were recorded while the CO partial pressure was increased up to several hPa. Fig. 9 shows the typical evolution of spectra in the CO stretching regime.

At least three distinct bands could be identified, at 2180, 2157, and 2144 cm^{-1}. The band at the lowest frequency develops only at high partial pressures and is typical of weak and unspecific adsorption of CO.

The band at ca. 2180 cm^{-1} is assigned to linear adsorption of CO on coordinatively unsaturated (cus) Mg^{2+} sites. The position of the band remains constant over a significant range of CO partial pressures and thus CO coverage, which suggests that there is no coupling between the CO oscillators. Indeed, on a highly hydrated surface as this one, it is expected that the concentration of cus Mg^{2+} is small and the sites are far apart. On MgO surfaces, the ad-

sorption of CO on Mg^{2+} ions is known to lead to a number of different bands depending on the coordination of the ions as discussed above. The Lewis acidity of the cus Mg^{2+} site on MgF$_2$-71 thus exhibits a strength comparable to that of low coordinated sites on MgO, specifically the strength seems to be higher than that of fourfold but lower than that of threefold coordinated sites. Tricoordinated sites on MgO only become available after dehydration at 500−805 K [24]; hence it can be considered unusual to find Lewis acid sites of such high strength after evacuation at room temperature. Dehydration of MgF$_2$-71 at 373 K and subsequent CO adsorption produces two instead of one band around 2180 cm^{-1}. This result indicates that there are at least two different environments of cus Mg^{2+} ions on the surface of MgF$_2$-71. This could be a result of the presence of Mg(F$_{6-x}$O$_x$) octahedra (Fig. 7a) or the interaction of a Mg-OH-group with a Lewis acid site (Fig. 7b). As a consequence of both effects the Lewis acid site should be weaker, resulting in a lower blue shift.

The band at 2157 cm^{-1} is assigned to the interaction of CO with OH groups. Fig. 10 shows how the band intensity of an OH group absorbing at about 3700 cm^{-1} decreases with increasing CO partial pressure. The band's position and its sharpness correspond to properties of bands reported for OH groups on MgO and Mg(OH)$_2$ [32]. It follows that the band at 3700 cm^{-1} represents OH groups bound to Mg^{2+}. The exact coordination and environment cannot be deduced since even for MgO assignment of this and other OH bands are debated [33].

Comparison of the spectra in Figs. 9 and 10 shows that the evolution of the band at 2157 cm^{-1} parallels the disappearance of the OH band. The carbonyl band position is in the range of CO adsorbed on OH groups. Unfortunately, the high degree of hydration and the resulting poor quality of the spectra in the OH regime obscure the position of the band of the disturbed OH groups. A shift, which would allow a statement on the acidity of these OH groups, can thus not be determined.
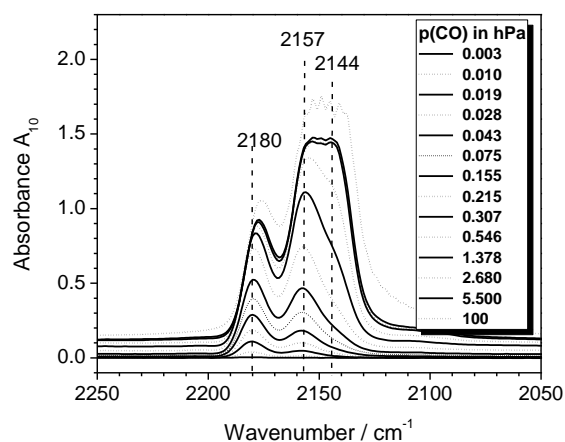

Fig. 9: Difference IR spectra of the carbonyl stretching region recorded during CO adsorption at 77 K on MgF$_2$-71 activated for 24 h at RT in vacuo.

Sol-gel prepared nanoscopic metal fluorides – a new class of tunable acid-base catalysts, S. Wuttke et al.., Catalysis Today 152 (2010), 2-10
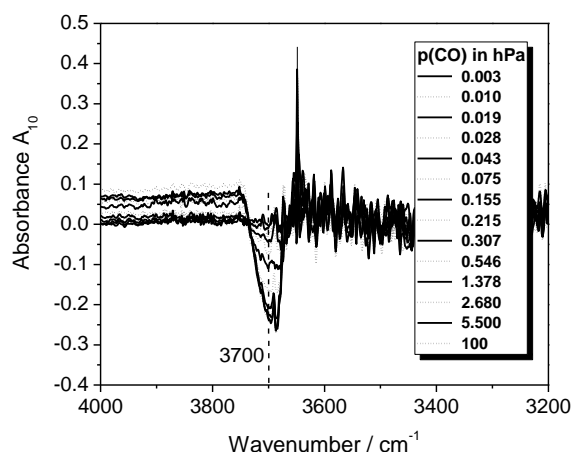
9

Fig. 10: Difference IR spectra of the OH stretching region recorded during CO adsorption at 77 K on MgF_2-71 activated for 24 h at RT in vacuo.

Fig. 11: The synthesis of (all-*rac*)-α-tocopherol through the condensation of 2,3,6-trimethylhydroquinone (TMHQ) with isophytol (IP).

However, Zaki and Knözinger [26] reported that the OH groups of MgO were not perturbed through exposure to CO at 77 K; the corresponding carbonyl bands of metal OH-CO complexes between 2150–2160 cm^{-1} were also absent in the spectra. Hence, strongly basic OH groups do not interact with CO. In turn, the CO affinity evidenced through the spectra in Figs. 9 and 10 demonstrates that the OH groups must be acidic in nature. Skocart et al. [34] investigated fluorinated alumina and found that, with increasing fluoride content, basic OH groups are substituted by fluoride, acidic OH groups are retained, and new, more strongly acidic OH groups are formed. In light of these findings it is conceivable that Mg-OH groups present on the surface of MgF_2-71 are acidic. This conclusion is further supported by the catalytic properties of the material.

It has been established that acidic halides, which are typically Lewis acids, have little or no activity for alkylation when used in a pure state. They can be activated by the addition of low concentrations of co-catalysts which interact with the Lewis acids to generate actual or potential Brønsted sites [35]. Because of their dual Lewis/Brønsted acidic character, we chose to test the hydroxylated magnesium fluoride in the synthesis of (all-*rac*)-α-tocopherol, which involves two reaction steps, the first one being the Friedel-Crafts alkylation of trimethylhydroquinone (TMHQ) with isophytol (IP) (Fig. 11). From a chemical and biological point of view, α-tocopherol is the most active form of Vitamin E group [36-37]. This reaction is not only a good test for the acid site types but is also interesting from an economical point of view, due to the high market demand for this compound and the various environmental problems that industry faces with the currently used homogeneous catalysts.

As we have already shown before, the hydroxylated magnesium fluorides are highly active and selective in the (all-*rac*)-α-tocopherol synthesis [23]. Further optimisation of the reaction conditions significantly improves the yield to (all-*rac*)-α-tocopherol. The most representative results
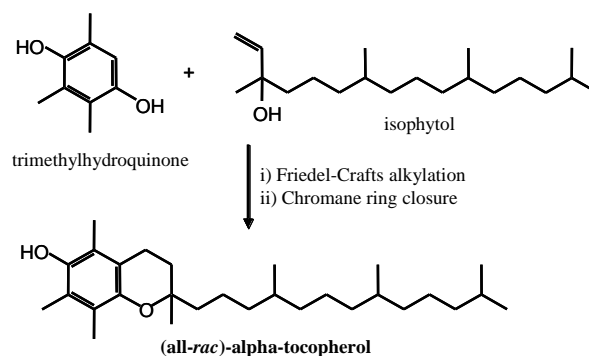
obtained in this synthesis, in the presence of hydroxylated fluorides are given in Table 1.

Further optimisation of the reaction conditions improved the yield and selectivity towards (all-*rac*)-α-tocopherol significantly (Table 1). In contrast to the catalytic conditions used previously [23] we added the fourfold mass of catalyst to the reaction mixture. The reaction is quite fast, after 1 h the conversion is 100 % and the selectivity is high. The only detected by-product formed in small amounts (5 – 10 %) was phytadiene, obviously due to the IP dehydration (Fig. 12). The separation of (all-*rac*)-α-tocopherol and phytadiene is difficult [36], and hence, the formation of this by-product must be avoided. On the basis of these results we carried out the reaction with an excess of trimethylhydroquinone and less catalyst material. As Table 1 shows, the yields of tocopherol are high and vary as a function both of the acidic sites nature and of the Lewis/Brønsted acid sites ratio. Therefore, samples with almost only Lewis sites are practically non-active while a sample with a high amount of very weak Brønsted sites resulted in a decrease in the tocopherol yield (Table 1, entries 1 and 7). An optimal combination of both types of acidic sites seems to be present on the surface of MgF_2-71 sample (Table 1, entries 3 and 4). As was expected an increase of the catalyst amount in the reaction mixture led to a great increases of the reaction rate (Table 1, entries, 2, 4 and 6).

Table 1: The influence of the key superficial features and the reaction parameters on the catalytic performances.

Entry	Catalyst	Number of A.C./m^2	IP/cat. molar ratio	Time/min	Yield of tocopherol/%
1	MgF_2-87	4.8×10^{17}	15	360	0
2	MgF_2-71	3.6×10^{17}	31	60	92.6
3[a]	MgF_2-71	3.6×10^{17}	123	180	>99.9
4	MgF_2-57	6.6×10^{17}	19	60	91.0
5[a]	MgF_2-57	6.6×10^{17}	76	180	83.3
6	MgF_2-40	5.4×10^{17}	30	60	87.7
7[a]	MgF_2-40	5.4×10^{17}	119	180	67.6
8	MgF_2-20	5.6×10^{17}	29	360	0

Reaction conditions: 200 mg of catalyst; T=100°C; TMHQ/IP=1/1; solvent: heptane/propylene carbonate=50/50 (v/v). Conversion is based on IP (C=100%). A.C.=acidic centres.
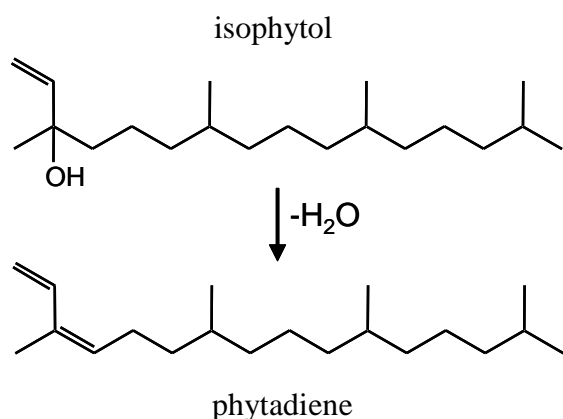[a] 50 mg of catalyst and TMHQ/IP=2/1.

Sol-gel prepared nanoscopic metal fluorides – a new class of tunable acid-base catalysts, S. Wuttke et al.,
Catalysis Today 152 (2010), 2-10

10

isophytol

-H$_2$O

phytadiene

Fig. 12: Formation of phytadiene from isophytol.

The other sample MgF$_2$-20 is totally inactive because of the absence of Brønsted acid sites and the presence of Brønsted basic sites. Suspensions of MgF$_2$-71, MgF$_2$-57 and MgF$_2$-40 in water turn the colour of indicator paper to red whereas the sample MgF$_2$-20 gives a pale blue colour. Due to the high amount of water, more OH-groups are at the surface and in the bulk, therefore the effects described in Fig. 7 become less relevant and typical OH-groups like in MgO are formed. This will be a matter of further investigation.

A problem with which this type of synthesis is generally confronted is the formation of many by-products [38-39], as phytadienes (because of the easy dehydration of IP in the presence of acids, Fig. 12 [40]), quinones (formed in the presence of traces of oxygen in the reaction system [9, 41]) and chromene (formed through a quinone-chromene rearrangement equilibrium, in the presence of basic centers [42]). These by-products lead to a decreased yield of tocopherol, and a decreased atom economy of the reaction. For this reason, one of the important issues in agreement with the green chemistry principles and sustainable development is to avoid their formation. If we take in consideration that in the case of (all-*rac*)-α-tocopherol synthesis, the presence of any by-product creates problems with its purification [36], this issue is even more important. Therefore, special precautions are also claimed for the synthesis of tocopherol such as, e.g., the synthesis has to be conducted under a stream of an inert gas and IP has to be dropwise added to the reaction media [43]. Contrarily, in the presence of these catalysts no quinone or/and chromene was detected even if reactions were conducted in atmospheric medium. No limitation is therefore imposed on the environment for the reaction in this case. The only detected by-product, formed in small amounts (5-10%), was phytadiene, due to the IP dehydration. The optimisation of the reaction conditions made possible to avoid the formation of this only by-product and to obtain pure tocopherol. Again, contrary to literature data which sometimes claim an excess of IP to improve the yield to tocopherol [44], in conditions used in this work, a decrease of the TMHQ/IP ratio from 1/1 to 1/2

favours the dehydration of IP (not shown in Table 1). To obtain pure tocopherol the reaction had to be conducted at 100 °C, with an excess of TMHQ (TMHQ/IP =2/1, Table 1, entry 3).

4. Conclusion

In summary it was demonstrated that metal oxofluorides exhibiting varying Brønsted/Lewis characteristics can be prepared by combining the fluorolytic with the hydrolytic sol-gel synthesis. If these two reaction types of metal alkoxides with understoichiometric amounts of anhydrous HF and water are performed consecutively, metal oxide fluorides with varying fluoride to hydroxide ratios can be prepared which exhibit both, Brønsted base and Lewis acid sites of different strengths. Thus, tuned solid base catalysts can be prepared showing excellent activities and selectivities in Michael additions as has been already demonstrated [15]. On the other hand, if the reaction of a metal alkoxide with stoichiometric amounts of HF in the simultaneous presence of water is performed as competitive fluorolysis/hydrolysis reaction partly hydroxylated MgF$_2$ phases carrying Lewis and Brønsted acid sites are obtained. These materials were successfully applied as heterogeneous catalysts in the (all-*rac*)-α-tocopherol synthesis. Fine tuning of their acidic properties made it possible to obtain a material which exhibits the right combination of Lewis/Brønsted acid sites for an optimum in catalytic properties. Keeping in mind that the fluorolytic sol-gel synthesis produces pure Lewis acidic metal fluorides or mixed metal fluorides with different strengths, based on this new fluorolytic sol-gel route a new class of tuneable acid-base catalysts has been introduced as summarised in Fig. 13.
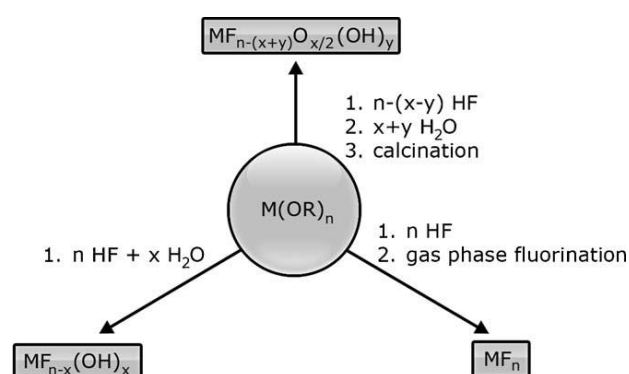

Fig. 13: Pathways of the different sol-gel-approaches towards metal fluorides with tunable acid-base surface sites.

Sol-gel prepared nanoscopic metal fluorides – a new class of tunable acid-base catalysts, S. Wuttke et al.,
Catalysis Today 152 (2010), 2-10

11

Acknowledgements

References

[1]   L.L. Hench and J.K. West, Chem. Rev., 90 (1990) 33.

[2]   H.K. Schmidt, Chemie in unserer Zeit, 3 (2001) 176.

[3]   E. Kemnitz, U. Groß, S. Rüdiger, C. S. Shekar, Angew. Chem., 115 (2003) 4383; Angew. Chem. Int. Ed., 42 (2003) 4251.

[4]   S. Rüdiger and E. Kemnitz, Dalton Trans., (2008) 1117.

[5]   T. Krahl, A. Vimont, G. Eltanany, M. Daturi and E. Kemnitz, J. Phys. Chem. C, 111 (2007) 18317.

[6]   S. Rüdiger, G. Eltanany and E. Kemnitz, J. Sol-Gel Sci Techn, 41 (2007) 299.

[7]   M. N.-Amiry, G. Eltanany, S. Wuttke, S. Rüdiger, E. Kemnitz, J.M. Winfield, J. Fluorine Chem., 129 (2008) 366.

[8]   S. Wuttke, G. Scholz, S. Rüdiger and E. Kemnitz, J. Mater. Chem., 17 (2007) 4980.

[9]   S.M. Coman, S. Wuttke, A. Vimont, M. Daturi and E. Kemnitz, Adv. Synth. Catal., 350 (2008) 2517.

[10]   S.M. Coman, P. Patil, S. Wuttke and E. Kemnitz, Chem. Commun., (2009) 460.

[11]   K. Tanabe, Bull. Chem. Soc. Jpn., 47 (1974) 1064.

[12]   E. Kemnitz, Y. Zhu and B. Adamczyk, J. Fluorine Chem., 114 (2002) 163.

[13]   J.K. Murthy, U. Gross, S. Rüdiger, E. Ünveren, W. Unger and E. Kemnitz, Appl. Catal. A, 282 (2005) 85.

[14]   J.K. Murthy, U. Gross, S. Rüdiger, and E. Kemnitz, Appl. Catal. A, 278 (2004) 133.

[15]   H.A. Prescott, Z.-J. Li, E. Kemnitz, J. Deutsch and H. Lieske, J. Mater. Chem., 15 (2005) 4616.

[16]   G. Spoto, E.N. Gribov, G. Ricchiardi, A. Damin, D. Scarano, S. Bordiga, C. Lamberti, A. Zecchina, Prog. Surf. Science, 76 (2004) 71.

[17]   J.C. Lavalley, Cat. Today, 27 (1996) 377.

[18]   J.I. Di Cosimo, V.K. Diez, M. Xu, E. Iglesia, C.R. Apesteguia, J. Catal., 178 (1998) 499.

[19]   J.A. Lercher, C. Colombier, H. Noller, J. Chem. Soc. Faraday Trans. 1, 80 (1984) 949.

[20]   E. Knözinger, K.-H. Jacob, S. Singh, P. Hofmann, Surf. Science, 290 (1993) 388.

[21]   C. Chizallet, G. Costentin, M. Che, F. Delbecq, P. Sautet, J. Am. Chem. Soc., 129 (2007) 6442.

[22]   S. Rüdiger, U. Groß, E. Kemnitz, J. Fluorine Chem., 128 (2007) 353-368.

[23]   S. Wuttke, S.M. Coman, G. Scholz, H. Kirmse, A. Vimont, M. Daturi, S.L.M. Schroeder, E. Kemnitz, Chem. Eur. J., 14 (2008), 11488.

[24]   C. Chizallet, G. Costentin, M. Che, F. Delbecq, P. Sautet, J. Phys. Chem. B, 110 (2006) 15878.

[25]   S. Mukhopadhyay, C.L. Bailey, A. Wander, B.G. Searle, C.A. Muryn, S.L.M. Schroeder, R. Lindsay, N. Weiher, N.M. Harrison, Surf. Science, 601 (2007) 4433.

[26]   M. I. Zaki, H. Knözinger, Mat. Chem. Phys., 17 (1987) 201.

[27]   H. Knözinger, P. Ratnasamy, Catal. Rev.-Sci. Eng., 17 (1978) 31.

[28]   H. Eckert, J.P. Yesinowski, L.A. Silver, E.M. Stolper, J. Phys. Chem., 92 (1988) 2055.

[29]   C. Chizallet, G. Costentin. H. L.-Pernot, M. Che, C. Bonhomme, J. Maquet, F. Delbecq, P. Sautet, J. Phys. Chem. C, 111 (2007) 18279.

[30]   S. Wuttke, G. Scholz, E. Kemnitz, unpublished results.

[31]   J.A. Lercher, C. Gründling, G.E.-Mirth, Cat. Today, 27 (1996) 353.

[32]   S. Coluccia, S. Lavagnino, L. Marchese, Mat. Chem. Phys., 18 (1988) 445.

[33]   E. Knözinger, K.-H. Jacob, S. Singh, P. Hofmann, Surface Science 290 (1993) 388-402

[34]   P.O. Scokart, S. A. Selim, J.P. Damon, P.G. Rouxhet, J. Col. Inter. Science, 70 (1979) 209.

[35]   M. C. Clark, C. Morris Smith, D. L. Stern, J. S. Beck, in Handbook of Heterogeneous Catalysis. Second, Completely revised and Enlarged Edition., G. Ertl, H. Knözinger, F. Schüth, J. Weitkamp (Eds.), WILEY-VCH Verlag GmbH & Co. KGaA, 7 (2008) 3153.

[36]   T. Netscher, Vitamins and Hormones, 76 (2007) 155.

[37]   A. Hasegawa, K. Ishihara, H. Yamamoto, Angew. Chem. Int. Ed., 42 (2003) 5731.

[38]   W. Bonrath, C. Dittel, L. Giraudi, T. Netscher, T. Pabst, Catal. Today., 121 (2007) 65.

[39]   S. Wang W. Bonrath, H. Pauling, F. Kienzle, J. of Supercritical Fluids, 17 (2000) 135.

[40]   M.B. Tarabrin, G.G. Shestakov, R. P. Evstigneeva, E. Yu. Bulychev, Pharm. Chem. J., 18 (1984) 572.

[41]   J. Greene, D. McHale, J. Chem. Soc., (1965) 5060.

[42]   K. A. Parker, T. L. Mindt, Org. Lett., 3 (2001) 3875.

[43]   H. Wang, B.-Q. Xu, Appl. Catal. A: General, 275 (2004) 247.

[44]   M. Matsui, N. Karibe, K. Hayashi, H. Yamamoto, Bull. Chem. Soc. Jpn., 68 (1995) 3569.